

Cite this: DOI: 00.0000/xxxxxxxxxx

## Phase stability in nickel phosphides at high pressures

Talgat M. Inerbaev,<sup>\*ab</sup> Nursultan Sagatov,<sup>ac</sup> Dinara Sagatova,<sup>ac</sup> Pavel N. Gavryushkin,<sup>ac</sup> Abdirash T. Akilbekov,<sup>b</sup> and Konstantin D. Litasov<sup>de</sup>

Received Date

Accepted Date

DOI: 00.0000/xxxxxxxxxx

We performed first-principles calculations on the crystal structure prediction and relative thermodynamic stability for Ni–P binary system at 100–400 GPa pressure range. The existence of seven new crystal structures is predicted. Six new crystals are isomorphic to the face-centered Ni crystal and pass into it when phosphorus atoms are replaced by nickel atoms. For Ni<sub>3</sub>P nickel phosphide, a new high-pressure phase of the *Cmca* space group was found. For the Ni<sub>2</sub>P compound at high pressures, the lattice stability of the allabogdanite structure is predicted. The *P*–*T* phase diagrams of Ni<sub>2</sub>P and Ni<sub>3</sub>P phosphides were calculated by the lattice dynamics method in the quasi-harmonic approximation.

## Introduction

Phosphides play a significant role in the mineralogy of iron meteorites as the components of the ternary Fe–Ni–P system. Although being rare, accessory minerals with composition (Fe,Ni)<sub>x</sub>P, they give important information about phosphorus geochemistry on the early stages of the universe formation.<sup>1–10</sup> The occurrence of these minerals in meteoritic samples is believed to originate either from the equilibrium condensation of protoplanetary materials taking place in the solar nebulae or from crystallization processes in the cores of parent bodies.

Iron-rich end-members of Fe–P system were intensively studied using both experimental and theoretical techniques. So far, most of the high-pressure investigations on iron phosphides have been restricted on Fe<sub>4</sub>P,<sup>11</sup> Fe<sub>3</sub>P,<sup>12</sup> Fe<sub>2</sub>P<sup>13,14</sup>, and FeP.<sup>15</sup> Several structural and magnetic phase transitions have been revealed as the result. Dera et al. observed that on heating at 8 GPa phase of Fe<sub>2</sub>P transforms to a high-pressure modification, which could be quenched to ambient conditions.<sup>13</sup> Theoretical modelling demonstrates that the stable phase of Fe<sub>2</sub>P should be the *Pnma* with the lowest total energy in the low pressure region, and the *P6̄2m* and *Pnma* phases would transform to the *P3̄m* phase with larger coordination number of iron at 125 GPa and 153 GPa, respectively.<sup>14</sup> Theoretical studies have shown

that Fe<sub>3</sub>P could decompose into Fe<sub>2</sub>P and Fe<sub>4</sub>P at pressures higher than 214 GPa<sup>16</sup>, and Fe<sub>3</sub>P and Fe would react with formation of Fe<sub>4</sub>P at ~100 GPa.<sup>11</sup> Fe<sub>3</sub>P exhibits a structural phase transition from *I4* to *P4/mnc* at 64 GPa and 1600 K accompanied with an electronic state transition from high-spin to low-spin at around 20–40 GPa.<sup>17,18</sup> Upon compression, Fe<sub>4</sub>P undergoes transition from ferromagnetic to nonmagnetic state at 80 GPa.<sup>11</sup> Britvin et al. reported two new structures of FeP (*Pnma*) and FeP<sub>2</sub> (*Pnnm*), found in the pyrometamorphic rocks.<sup>8,9</sup>

Alloying effect of Ni on physical properties and structure of Fe and it's alloys with light elements is also of geological interest, as according to geochemical assesment Earth's core could contain up to 10mol% of Ni (Уточнить и поставить ссылку на Чёрную Книжку (?)). Addition of nickel to iron phosphides affect the structure and phase stability. The example of Fe<sub>2</sub>P shows, that even a small addition of Ni and Co stabilise the structure of alabogdanite against XXX<sup>3,4,19</sup>, and also slightly increases the bulk modulus of the alabogdanite phase.<sup>19</sup> А может здесь сослаться на нашу статью по алабогданиту (Bekker, Sagatov et al., 2020)? The incorporation of Ni in nonmagnetic Fe<sub>4</sub>P results in reduction of the compressional and shear wave velocities enhancing their anisotropy.<sup>11</sup>

There are numerous phases were revealed in Ni–P system at ambient pressure. Among them are Ni<sub>3</sub>P, Ni<sub>8</sub>P<sub>3</sub>, Ni<sub>12</sub>P<sub>5</sub>, Ni<sub>2</sub>P, Ni<sub>5</sub>P<sub>4</sub>, NiP, NiP<sub>2</sub>, and NiP<sub>3</sub>. Вижу здесь NiP<sub>3</sub>, Ni<sub>5</sub>P<sub>4</sub>, Ni<sub>12</sub>P<sub>5</sub>. Возникает вопрос, а почему мы их на выпуклую оболочку не нанесли? Ni<sub>8</sub>P<sub>3</sub> и NiP<sub>2</sub> нанесли, а эти нет? Какой принцип для выбора фаз? По-хорошему следовало бы для всех этих составов провести предсказания, как мы это делали с гидридами. В Методику нужно обязательно добавить, что какие-то фазы мы брали из литературных данных и просто протягивали их по давлению. Подумайте,

<sup>a</sup> Sobolev Institute of Geology and Mineralogy, Siberian Branch of the Russian Academy of Sciences, Novosibirsk, 630090 Russia. E-mail: inerbaevtm@igm.nsc.ru

<sup>b</sup> L. N. Gumilyov Eurasian National University, Nur-Sultan, 010008 Kazakhstan.

<sup>c</sup> Novosibirsk State University, Novosibirsk, 630090 Russia.

<sup>d</sup> Vereshchagin Institute for High Pressure Physics, Russian Academy of Sciences, Moscow, 108840, Russia.

<sup>e</sup> Fersman Mineralogical Museum Russian Academy of Sciences, Moscow, Russia.

Table 1 Structural data for the found phases of Ni–P system –(1) Здесь необходимо привести данные предсказанного аллабогданита-Ni<sub>2</sub>P, чтобы желающие могли убедиться что это действительно аллабогданит. Параметры ячейки могут пригодиться экспериментаторам для расшифровки дифрактограмм. Вообще привести стоит. – (2) Параметры ячейки лучше округлить до тысячных, четвёртая цифра абсолютно не значима. Координаты атомов – до десятичных (именно так делает большинство авторов, например К. Пикард, лично я бы всё до тысячных округлял)) – (3) С помощью функции multirow можно сделать, чтобы названия Phase, Pressure и пр., были в центре ячейки – (4) В ячейке Lattice parameters в скобках указано (Å, degree), а потом в таблице снова стоят Å– (5) Структурные данные лучше приводить для наиболее низкого давления (в поле стабильности, конечно), потому что при 400 ГПа эксперименты никто ставить не будет. И данные лучше приводить для одного и того же давления, чтобы можно было сравнить объёмы. Вообще, все твёрдые растворы лучше привести на 100 ГПа.

Phase	Pressure (GPa)	Space group	Lattice parameters (Å, degree)			Atomic coordinates			
						Atom	x	y	z
Ni <sub>14</sub> P	400	C2/m (#12)	$a=6.8686\text{Å}$ $\alpha=90$	$b=6.2097\text{Å}$ $\beta=119.559$	$c=5.0749\text{Å}$ $\gamma=90$	Ni1	0.00000	0.16860	0.00000
						Ni2	0.09850	0.00000	0.39699
						Ni3	0.30065	0.00000	0.19837
						Ni4	0.70280	0.33474	0.80023
						Ni5	0.59887	0.16587	0.39807
						P1	0.00000	0.50000	0.00000
Ni <sub>12</sub> P	400	R $\bar{3}$ (#148)	$a=7.4609\text{Å}$ $\alpha=90.00$	$b=7.4609\text{Å}$ $\beta=90.00$	$c=5.0755\text{Å}$ $\gamma=120$	Ni1	0.53902	0.38422	0.00134
						Ni2	-0.02851	0.40876	0.33153
						P1	0.00000	0.00000	0.00000
Ni <sub>10</sub> P	300	P $\bar{1}$ (#2)	$a=3.6654\text{Å}$ $\alpha=107.482$	$b=4.7295\text{Å}$ $\beta=104.937$	$c=4.7339\text{Å}$ $\gamma=97.456$	Ni1	0.04502	0.41007	0.18032
						Ni2	0.59015	0.31912	0.35915
						Ni3	0.13716	0.22851	0.54678
						Ni4	0.22672	0.04944	-0.09103
						Ni5	0.67759	0.13805	0.72806
						P1	0.50000	0.50000	0.00000
Ni <sub>8</sub> P	200	P $\bar{1}$ (#2)	$a=3.7669\text{Å}$ $\alpha=75.00$	$b=3.7719\text{Å}$ $\beta=82.569$	$c=4.8694\text{Å}$ $\gamma=80.481$	Ni1	0.22148	0.11048	0.56082
						Ni2	0.67093	0.33311	0.66740
						Ni3	0.44401	0.21845	0.11085
						Ni4	0.11116	0.55650	0.78047
						P1	0.00000	0.00000	0.00000
Ni <sub>7</sub> P	100	P $\bar{1}$ (#2)	$a=3.7553\text{Å}$ $\alpha=73.032$	$b=3.7772\text{Å}$ $\beta=89.980$	$c=4.3925\text{Å}$ $\gamma=79.849$	Ni1	0.50201	0.00029	0.24766
						Ni2	0.00000	0.00000	0.50000
						Ni3	0.75389	0.49840	0.12435
						Ni4	0.24895	0.50693	0.37130
						P1	0.00000	0.00000	0.00000
Ni <sub>5</sub> P	200	P6 <sub>3</sub> /mcm (#193)	$a=3.7732\text{Å}$ $\alpha=90.00$	$b=3.7732\text{Å}$ $\beta=90.00$	$c=7.0786\text{Å}$ $\gamma=120$	Ni1	0.33333	0.66667	0.00000
						Ni2	0.67096	0.00000	0.25000
						P1	0.00000	0.00000	0.00000
Ni <sub>3</sub> P	100	Cmca (#64)	$a=13.1666\text{Å}$ $\alpha=90.00$	$b=4.4854\text{Å}$ $\beta=90.00$	$c=4.4851\text{Å}$ $\gamma=90.00$	Ni1	0.38137	0.00000	0.00000
						Ni2	0.00000	0.18176	0.81801
						Ni3	0.25000	0.74729	0.25000
						P1	0.13651	0.00000	0.00000
Ni <sub>2</sub> P	100	Pnma (#64)	$a=4.271\text{Å}$ $\alpha=90.00$	$b=3.307\text{Å}$ $\beta=90.00$	$c=6.247\text{Å}$ $\gamma=90.00$	Ni1	0.4537	0.25	0.7890
						Ni2	0.8260	0.25	0.0589
						P1	0.8021	0.25	0.3870

может имеет смысл запустить эти расчёты на предсказание, пока статья будет на рецензии они досчитаются и мы это включим в статью However, the data on this system at high-pressures, especially above 100 GPa, are limited. Donohue et al.<sup>20</sup> studied P-rich compositions (NiP<sub>2.2–2.5</sub>) at 1.5–6.5 GPa. Dera et. al.<sup>21</sup> synthesized a cubic NiP<sub>2</sub> phase at 6.5 GPa during heating at 1200°C and subsequent cooling to 900°C. Incongruent melting associated with formation of pyrite-type NiP<sub>2</sub> and amorphous Ni–P alloy was found at an intermediate pressure range, between 6.5 and 40 GPa. The phase transitions in Ni<sub>2</sub>P were not observed in these experiments at pressures up to 50 GPa consistently with theoretical predictions.<sup>19</sup> Several reversible phase transitions were established in NiP at ambient temperature: (a) from *Pbca* to *Cmc2*<sub>1</sub> at 3.5 GPa, (b) to *Pnma*-phase at 8.5 GPa and to another *Cmc2*<sub>1</sub>-phase, but with different crystal structure at 25 GPa.<sup>22,23</sup> Litasov et.al. studied

the melting processes and subsolidus phase relations in the Ni–Ni<sub>2</sub>P system at 6 GPa and 900–1600°C.<sup>24</sup> Хорошо бы в этой и других подобных ссылках отметить конкретный результат. А так получается просто констатация факта, что кто-то что-то исследовал. А что получено в результате? The stability of four intermediate compositions, Ni<sub>3</sub>P, Ni<sub>8</sub>P<sub>3</sub>/Ni<sub>5</sub>P<sub>2</sub>, Ni<sub>12</sub>P<sub>5</sub>, and Ni<sub>2</sub>P transjordanite was found. The Ni<sub>12</sub>P<sub>5</sub> phase becomes unstable at 900°C and decomposes into Ni<sub>5</sub>P<sub>2</sub> and Ni<sub>2</sub>P.

The phase stability, elastic properties, hardness and related electronic structures of Ni–P crystal phases at ambient pressure and zero temperature were studied theoretically in Ref.<sup>25,26</sup>. The equations of state and structural parameters of Ni<sub>2</sub>P, NiP<sub>2</sub> (pyrite type) and Ni-doped Fe<sub>2</sub>P (allabogdanite) at high pressures were determined with first-principles calculations.<sup>19</sup> There was not found barringerite-allabogdanite phase transition in Ni<sub>2</sub>P at pressures up to 50 GPa. Bulk modulus of (Fe<sub>1–x</sub>Ni<sub>x</sub>)<sub>2</sub>P

(allabogdanite) increases with Ni concentration. Increasing the concentration of Ni decreases the stability of structure and suppresses the total magnetic moment of the system.

In present research, we theoretically investigate Ni-P compounds in the pressure range from 100 to 400 GPa. A search for new crystalline structures is carried out. The relative stability of all predicted and well-known experimentally observed structures of the Ni-P system is investigated. The phase diagram of the Ni<sub>2</sub>P system is calculated, where barringerite-allobogdanite structural phase transition occurs at pressures of 77-87 GPa depending on temperature. Similar calculations of the phase equilibrium between the new high-pressure Ni<sub>3</sub>P phase and the schreibersite structure are also performed.

## Computation Details

The structure predictions were performed using USPEX code based on evolutionary algorithms<sup>27–29</sup> and AIRSS based on a random sampling method.<sup>30,31</sup> Crystal structure prediction calculations were divided into two stages. At the first stage, the search for stable structures of intermediate compositions was performed using the USPEX package. At the second stage, the predictions were performed for the fixed compositions represented on the convex hull constructed at the first stage using USPEX and AIRSS. При каких давлениях осуществлялись предсказания структур? В случае AIRSS для какого количества формульных единиц? Хорошо бы указать и сколько структур было просчитано. The calculations of the electronic structure were carried out within the DFT using the VASP 5.4 package.<sup>32,33</sup> The exchange-correlation interaction was taken into account in the generalized gradient approximation (GGA) in the form of the Perdew-Burke-Ernzerhof (PBE) functional<sup>34</sup> in a plane-wave basis set along with projector augmented-wave (PAW) pseudopotentials.<sup>35</sup> For all studied structures, calculations were performed, taking into account the spin polarization. It was found that in all cases, except for the new predicted phases Ni<sub>10</sub>P, Ni<sub>12</sub>P, and Ni<sub>14</sub>P, the magnetic moment is equal to zero. The computation parameters were as follows: energy cut-off – 450 eV; the density of the grid of Monkhorst-Pack k-point mesh –  $0.5\text{\AA}^{-1}$ . The most promising predicted structures were then optimized with higher accuracy at various pressures. In these calculations, the cut-off energy was 700 eV and the density of k-points was  $0.2\text{\AA}^{-1}$ . Тут, как уже было отмечено, нужно добавить про оптимизацию структур, взятых из литературных источников.

To take into account the temperature effect and predict the phase diagrams, we used the method of lattice dynamics within the quasi-harmonic approximation (QHA). For this task, the phonon frequencies were calculated with the PHONOPY code.<sup>36</sup> Ссылка на BECTy.

## Results and Discussion

The analysis of HP crystal structures

Structural data of the new phases predicted with USPEX and AIRSS codes are summarized in Table 1 and shown in Fig. 1. All found structures are dynamically stable, the correspond-

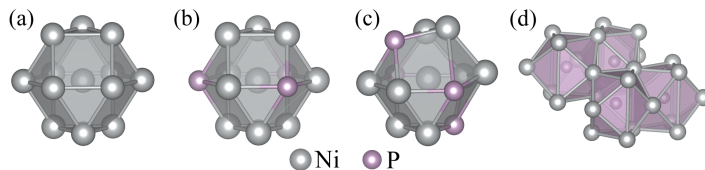


Fig. 1 Coordination polyhedrons in fcc-Ni (a), Ni<sub>5</sub>P (b), Ni<sub>3</sub>P (c), and Ni<sub>2</sub>P structures (d).

ing phonon spectra presented in Supporting Information (SI) Указать номер рисунка.

The structures of Ni<sub>14</sub>P, Ni<sub>12</sub>P, Ni<sub>10</sub>P, Ni<sub>8</sub>P, Ni<sub>7</sub>P, Ni<sub>5</sub>P, and Ni<sub>3</sub>P are characterized by *fcc* packing, with Ni atoms partially substituted by P atoms. The pure Ni also present in the *fcc* form up to 400 GPa. Thus, the found structures can be considered as (Ni,P) solid solutions. This type of isomorphism between *d*-metal and light element is unusual at ambient pressures. At extreme pressures of the Earth's core, when elements which are typical non-metals like sulfur adopt metallic properties<sup>37</sup>, this isomorphism became widespread. Isomorphic replacement of iron on S, Si and C within *hcp* or *bcc* crystal structures can be given as an example<sup>38</sup>. Я здесь в обоих случаях на себя ссылаюсь, хорошо бы добавить и другие ссылки (например на Cote и Vocadlo), но сходу ничего предложить не могу. P atoms in found structures tend to be homogeniously spread through the structure, without clustering or group formation.

Ni<sub>14</sub>P, Ni<sub>12</sub>P, Ni<sub>10</sub>P, Ni<sub>8</sub>P, Ni<sub>7</sub>P, Ni<sub>5</sub>P structures are characterised by almost ideal *fcc* packing, with both Ni-Ni and Ni-P bonds are of the same length, equal to 2.7 Å at 100 GPa. The Ni-Ni bond in the pure Ni is characterised by the same length. Ni<sub>3</sub>P structure is sufficiently deformed, as shown on Figure 1, the Ni-P bond is equal to 2.25 Å while length of Ni-Ni bonds vary in the range 2.25-2.35 Å. The found Ni<sub>2</sub>P-*Pnma* structure is the analogue of allabogdanite mineral with composition Fe<sub>2</sub>P. Allabogdanite is of cottunite-type, does not having close-packing of atoms, in contrast to *fcc* structure which is 3-layered close-packing. The calculations, which results will be presented below, show that experimentally synthesised at ambient pressure Ni<sub>8</sub>P<sub>3</sub> structure is also stable up to 400 GPa. As well as Ni<sub>2</sub>P, the structure of this phase are not of closed packing type. Thus, at nearly 25 mol.% of P content in (Ni,P) alloy, the change of the structural type takes place. This value can be accepted as the estimation for the phosphorus solubility in Ni structure at high pressures and low temperatures. As temperature increases the limits of isomorphism, this value can be sufficiently higher for the conditions of the cores of the Earth or planets. The fact, that similar isomorphism was not found in Fe-P systems, likely shows that solubility of P in (Fe,Ni) alloy will be higher than in the pure Fe.

Spin-polarized calculations show the presence of a magnetic moment in structures with a relatively high nickel content from Ni<sub>14</sub> to Ni<sub>8</sub>P, as shown in Fig. 2. In all other cases, the magnetic order is absent. The magnetic moment per nickel atom decreases with an increase in the specific phosphorus content in the system. With increasing pressure, the magnetic moment

and magnetic ordering completely disappear at a pressure of 315, 360, 350, and 115 GPa for the  $\text{Ni}_{14}\text{P}$ ,  $\text{Ni}_{12}\text{P}$ ,  $\text{Ni}_{10}\text{P}$ , and  $\text{Ni}_8\text{P}$  lattices, respectively. Unlike the considered phosphides, the magnitude of the magnetic moment in pure nickel weakly depends on external pressure. With an increase in pressure from 100 to 200 GPa, the magnetic moment per nickel atom decreases from  $0.58 \mu_B$  to  $0.5 \mu_B$  and then remains practically unchanged.

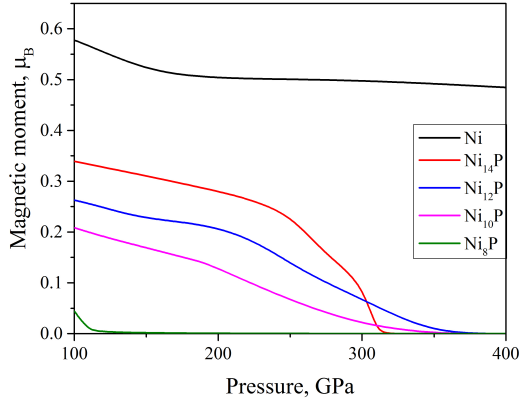


Fig. 2 Pressure dependence of magnetic moment (in Bohr magneton,  $\mu_B$ ) per Ni atom for predicted Ni-P crystal structures. The dependence of the magnetic moment on pressure for pure nickel is given for comparison.

#### Thermodynamic of Ni-P compounds

Both sets of the predicted and experimentally observed Ni-P binary compounds were used to evaluate the formation enthalpy  $\Delta H$  with respect to the elemental solids Ni and P according to Eq. 1, in order to explore the thermodynamic stability of Ni-P:

$$\Delta H(\text{Ni}_n\text{P}_m) = \frac{H(\text{Ni}_n\text{P}_m) - nH(\text{Ni}) - mH(\text{P})}{Z(n+m)}, \quad (1)$$

where  $H = U + PV$  is the enthalpy of each compound,  $Z$  is a number of formula units in the unit cell of the structure and  $\Delta H$  is the enthalpy of formation per formula unit. Herein,  $U$ ,  $P$ , and  $V$  are internal energy, pressure and volume, correspondingly. Detailed information about the element solids can be found in SI. Ссылка на рисунок.

The relative stabilities of the considered compositions at the selected pressures of 100, 200, 300, and 400 GPa, with  $\Delta H$  evaluated per atom, are shown in the form of the co-called convex hull Fig. 3, useful for assessing of the phases thermodynamic stability. Points corresponding to the phases with enthalpy lower than the enthalpy of mechanical mixture of the neighbouring compounds forms the convex hull on such a plot. All points above the convex hull corresponds to the unstable phases, decomposing on the mixture of neighbouring compounds. In addition to the predicted and described above  $\text{Ni}_{14}\text{P}$ ,  $\text{Ni}_{12}\text{P}$ ,  $\text{Ni}_{10}\text{P}$ ,  $\text{Ni}_8\text{P}$ ,  $\text{Ni}_7\text{P}$ ,  $\text{Ni}_5\text{P}$ ,  $\text{Ni}_3\text{P}$ , and  $\text{Ni}_2\text{P}$  structures, we have also considered  $\text{Ni}_8\text{P}_3$  and  $\text{NiP}_2$  structures, synthesised experimentally at ambient pressure.

Predicted solid solutions  $\text{Ni}_{14}\text{P} - \text{Ni}_7\text{P}$  are stable within all

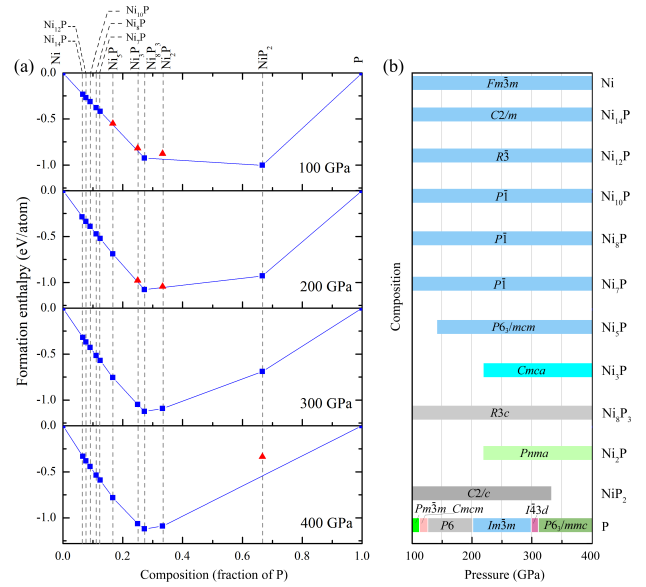


Fig. 3 Global stability convex hulls of the Ni-P system at the pressure range 100-400 GPa (a) and predicted pressure-composition phase diagram for the Ni-P system. Blue squares denote stable structures, red triangles - metastable structures.

pressure range from 100 to 400 GPa, while solid solution enriched with phosphorus are stabilised with pressure.  $\text{Ni}_5\text{P}$  became stable from 200 GPa and above, while  $\text{Ni}_3\text{P}$  from 300 GPa and above. Allabogdanite- $\text{Ni}_2\text{P}$  is also stabilised against decomposition at 200 GPa. Experimental phase  $\text{Ni}_8\text{P}_3$  is stable in all pressure range, while  $\text{NiP}_2$  destabilised above 300 GPa.

It has to be emphasized, that the results presented in Fig.3 are obtained neglecting thermal effects. In order to account for the effect of temperature on Gibbs energy, we use method of lattice dynamic. Within this method, it is necessary to calculate the vibrational spectra of all the structures considered. We performed phonon mode calculations for all predicted structures, described above. Experimentally synthesised  $\text{Ni}_8\text{P}_3$  was not considered in this context, due to the large size of the unit cell, containing 132 atoms. Speculatively we assume thermodynamic instability of such a low symmetric structure in the field of high temperatures, due to effect of entropy.

Due to natural occurrence of schreibersite- $\text{Ni}_3\text{P}$ , allabogdanite- $\text{Ni}_2\text{P}$ , and transjordanite- $\text{Ni}_2\text{P}$  phases and their findings in meteoritic rocks, we determined PT phase diagrams for these compounds, presented in Fig. 4. The diagrams shows, that transition from barringerite to allabogdanite structure in the  $\text{Ni}_2\text{P}$  system occurs in the pressure range 77-88 GPa at temperatures 0-2000 K. The transition from schreibersite to the found  $\text{Cmcm}$  structure occurs at 62 GPa and pressure of phase transition is almost independent from temperature.

#### Acknowledgements

The authors are thankful to the Center for Comput. Mater. Sci., Institute for Materials Research, Tohoku University and Novosibirsk University Supercomputing Center for their continuous support of the supercomputing system to be used for our

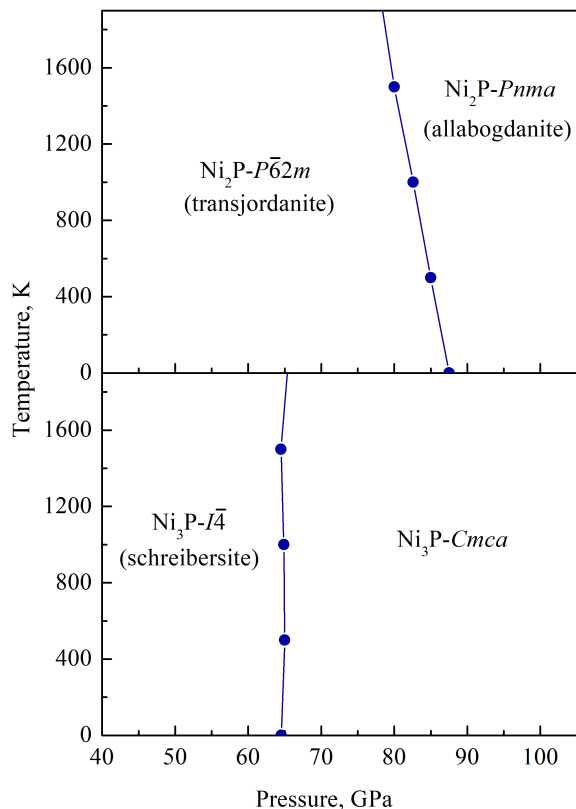


Fig. 4  $P$ - $T$  diagram of (a)  $\text{Ni}_2\text{P}$  and (b)  $\text{Ni}_3\text{P}$

simulation works.

The reported calculations on crystal structure prediction was funded by RFBR, project number 19-35-90043, calculations of  $PT$  diagrams – by the state assignment project of IGM, SBRAS.

## Notes and references

- 1 R. Skála and I. Čisářová, *Physics and Chemistry of Minerals*, 2005, 31, 721–732.
- 2 R. Skála and M. Drábek, *Mineralogical Magazine*, 2003, 67, 783–792.
- 3 P. R. Buseck, *Science*, 1969, 165, 169–171.
- 4 S. N. Britvin, N. S. Rudashevsky, S. V. Krivovichev, P. C. Burns and Y. S. Polekhovsky, *American Mineralogist*, 2002, 87, 1245–1249.
- 5 G. Pratesi, L. Bindi and V. Moggi-Cecchi, *American Mineralogist*, 2006, 91, 451–454.
- 6 S. J. B. Reed, *Mineralogical Magazine and Journal of the Mineralogical Society*, 1968, 36, 850–854.
- 7 Britvin Sergey N., Shilovskikh Vladimir V., Pagano Renato, Vlasenko Natalia S., Zaitsev Anatoly N., Krzhizhanovskaya Maria G., Lozhkin Maksim S., Zolotarev Andrey A. and Gurzhiy Vladislav V., *Scientific Reports*, 2019, 9, 1047.
- 8 S. N. Britvin, M. N. Murashko, Y. Vapnik, Y. S.

- Polekhovsky, S. V. Krivovichev, O. S. Vereshchagin, N. S. Vlasenko, V. V. Shilovskikh and A. N. Zaitsev, *Physics and Chemistry of Minerals*, 2019, 46, 361–369.
- 9 S. N. Britvin, Y. Vapnik, Y. S. Polekhovsky, S. V. Krivovichev, M. G. Krzhizhanovskaya, L. A. Gorelova, O. S. Vereshchagin, V. V. Shilovskikh and A. N. Zaitsev, *Mineralogy and Petrology*, 2019, 113, 237–248.
- 10 Britvin Sergey N., Murashko Mikhail N., Vapnik Yevgeny, Polekhovsky Yuri S., Krivovichev Sergey V., Vereshchagin Oleg S., Shilovskikh Vladimir V., Vlasenko Natalia S. and Krzhizhanovskaya Maria G., *Physics and Chemistry of Minerals*, 2020, 47, 3.
- 11 X. Wu, M. Mookherjee, T. Gu and S. Qin, *Geophysical Research Letters*, 2011, 38,.
- 12 H. P. Scott, S. Huggins, M. R. Frank, S. J. Maglio, C. D. Martin, Y. Meng, J. Santillán and Q. Williams, *Geophysical Research Letters*, 2007, 34,.
- 13 P. Dera, B. Lavina, L. A. Borkowski, V. B. Prakapenka, S. R. Sutton, M. L. Rivers, R. T. Downs, N. Z. Boctor and C. T. Prewitt, *Geophysical Research Letters*, 2008, 35,.
- 14 X. Wu and S. Qin, *Journal of Physics: Conference Series*, 2010, 215, 012110.
- 15 T. Gu, X. Wu, S. Qin and L. Dubrovinsky, *Physics of the Earth and Planetary Interiors*, 2011, 184, 154–159.
- 16 Z. Zhao, L. Liu, S. Zhang, T. Yu, F. Li and G. Yang, *RSC Adv.*, 2017, 7, 15986–15991.
- 17 T. Gu, Y. Fei, X. Wu and S. Qin, *Earth and Planetary Science Letters*, 2014, 390, 296–303.
- 18 T. Gu, Y. Fei, X. Wu and S. Qin, *American Mineralogist*, 2016, 101, 205–210.
- 19 J. Nisar and R. Ahuja, *Earth and Planetary Science Letters*, 2010, 295, 578–582.
- 20 P. C. Donohue, T. A. Bither and H. S. Young, *Inorganic Chemistry*, 1968, 7, 998–1001.
- 21 P. Dera, B. Lavina, L. A. Borkowski, V. B. Prakapenka, S. R. Sutton, M. L. Rivers, R. T. Downs, N. Z. Boctor and C. T. Prewitt, *Journal of Geophysical Research: Solid Earth*, 2009, 114,.
- 22 P. Dera, J. D. Lazarz and B. Lavina, *Journal of Solid State Chemistry*, 2011, 184, 1997–2003.
- 23 P. Dera, J. Nisar, R. Ahuja, S. Tkachev and V. B. Prakapenka, *Physics and Chemistry of Minerals*, 2013, 40, 183–193.
- 24 K. D. Litasov, A. F. Shatskiy, D. A. Minin, K. E. Kuper and H. Ohfuji, *High Pressure Research*, 2019, 39, 561–578.
- 25 J.-S. Chen, C. Yu, H. Lu and J.-M. Chen, *Phase Transitions*, 2016, 89, 1078–1089.
- 26 D. Zhao, L. Zhou, Y. Du, A. Wang, Y. Peng, Y. Kong, C. Sha, Y. Ouyang and W. Zhang, *Calphad*, 2011, 35, 284–291.
- 27 C. W. Glass, A. R. Oganov and N. Hansen, *Computer Physics Communications*, 2006, 175, 713–720.
- 28 A. R. Oganov and C. W. Glass, *The Journal of Chemical Physics*, 2006, 124, 244704.



- 29 A. O. Lyakhov, A. R. Oganov and M. Valle, *Computer Physics Communications*, 2010, 181, 1623–1632.
- 30 C. J. Pickard and R. J. Needs, *Phys. Rev. Lett.*, 2006, 97, 045504.
- 31 C. J. Pickard and R. J. Needs, *Journal of Physics: Condensed Matter*, 2011, 23, 053201.
- 32 G. Kresse and D. Joubert, *Phys. Rev. B*, 1999, 59, 1758–1775.
- 33 G. Kresse and J. Furthmüller, *Phys. Rev. B*, 1996, 54, 11169–11186.
- 34 J. P. Perdew, K. Burke and M. Ernzerhof, *Phys. Rev. Lett.*, 1997, 78, 1396–1396.
- 35 P. E. Blöchl, *Phys. Rev. B*, 1994, 50, 17953–17979.
- 36 A. Togo and I. Tanaka, *Scripta Materialia*, 2015, 108, 1–5.
- 37 P. N. Gavryushkin, K. D. Litasov, S. S. Dobrosmislov and Z. I. Popov, *physica status solidi (b)*, 2017, 254, 1600857.
- 38 P. N. Gavryushkin, Z. I. Popov, K. D. Litasov, A. B. Belonoshko and A. Gavryushkin, *Geophysical Research Letters*, 2016, 43, 8435–8440.
- 39 F. Jerems, C. M. Mahon, A. G. Jenner and R. D. Greenough, *Ferroelectrics*, 1999, 228, 333–341.